Research Paper https://doi.org/10.7733/jnfcwt.2020.18.4.481

A Study on Reusable Metal Component as Burnable Absorber Through Monte Carlo Depletion Analysis

Boravy Muth, Saed Alrawash, Chang Je Park*, and Jong Sung Kim
Sejong Univesity, 209, Neungdong-ro, Gwangjin-gu, Seoul, Republic of Korea

(Received September 28, 2020 / Revised October 21, 2020 / Approved November 18, 2020)

After nuclear power plants are permanently shut down and decommissioned, the remaining irradiated metal components such as stainless steel, carbon steel, and Inconel can be used as neutron absorber. This study investigates the possibility of reusing these metal components as neutron absorber materials, that is burnable poison. The absorption cross section of the irradiated metals did not lose their chemical properties and performance even if they were irradiated over 40-50 years in the NPPs. To examine the absorption capability of the waste metals, the lattice calculations of WH 17×17 fuel assembly were analyzed. From the results, Inconel-718 significantly hold-down fuel assembly excess reactivity compared to stainless steel 304 and carbon steel because Inconel-718 contains a small amount of boron nuclide. From the results, a 20wt% impurity of boron in irradiated Inconel-718 enhances the excess reactivity suppression. The application of irradiated Inconel-718 as a burnable absorber for SMR core was investigated. The irradiated Inconel-718 impurity with 20wt% of boron content can maintain and suppress the whole core reactivity. We emphasize that the irradiated metal components can be used as burnable absorber materials to control the reactivity of commercial reactor power and small modular reactors.

Keywords: Reusable metal components, Scrap metal, Irradiated Inconel-718, Burnable absorber, Monte Carlo simulation

*Corresponding Author.
Chang Je Park, Sejong University, E-mail: parkcj@sejong.ac.kr, Tel: +82-2-3408-4432

ORCID

Boravy Muth	http://orcid.org/0000-0002-1890-0643	Saed Alrawash	http://orcid.org/0000-0002-9268-8767
Chang Je Park	http://orcid.org/0000-0002-0278-721X	Jong Sung Kim	http://orcid.org/0000-0001-7349-074X

1. Introduction

In nuclear power plants (NPPs), every nuclear installation is limited to its lifetime and the decommissioning of NPPs should begin after nuclear reactor is permanently shut down. A large amount of low-level radioactive wastes such as concrete, steel and other valuable materials are generated from decommissioning. Some of the mentioned radioactive materials, especially metals, still have economic value, and it is beneficial to recycle and reuse them [1, 2]. Nuclear Energy Agency (NEA) published several reports regarding the recycle and reuse of material arising from the decommissioning of nuclear facilities [3, 4]. NEA reports are mainly focused on metals and also provide preceptive information through the organization of decommissioning activities. These decommissioning activities are involved in examining the health, environmental, and economic impact. In addition, the commissioning activities are also incorporated the technical adequacy and cost-effectiveness of available decontamination that is related with disposal and replacement of scrap metals, and comparison with a proposed "tiered" regulatory regime is also provided. These decommissioning activities would allow large portions of scrap metal materials to be recycled and reused. There are many thermal technologies to treat or process the waste production generated from nuclear power plants, nuclear fuel cycle facilities, and centralized radioactive waste processing facilities around the world [5]. These technologies are divided into three major parts (self-explanation of each technologies is given in ref [5]):

- Pre-treatment processes: processes whose end product requires further treatment; included pyrolysis, steam reforming, calcinations, sintering, thermochemical treatment, and molten salt oxidation.
- Treatment processes: processes change the characteristics of the waste and may result in an end product which is an appropriate waste form for disposition, such as incineration.
- Conditioning processes: processes result in an end product which is in a waste package suitable for handling, transport, storage and/or disposal. Vitrification, melting and plasma arc technologies are included in this category.

The thermal technologies mentioned can be used to recycle the contaminated metal generated by the decommissioning of NPP, depending on the regulations and the cost-effectiveness of the organization. In addition, a case study on Sweden's NPPs (Ringhals site 1 to 4) is described to estimate the total decommissioning cost, as well as to estimate of scrap metal production [6]. Table 1 lists the general information about the Ringhals NPP sites, including their reactor types, operating power and operating period. As can be seen from Table 1, only Ringhals 1 is BWR (Boiling Water Reactor), and the rest of Ringhals NPPs are PWR (Pressurizer Water Reactor). The total operation period of those reactors is 50 years while the expectation of those reactors to be permanently shut down and start decommissioning is in between 2019 and 2043. The report of Ringhals plants decommissioning cost is also to estimate the amount of metal wastes being generated. The estimated values of waste production from each sites are summarized in Table 2 [6]. The total metal waste of 31,075 metric tons is measured from Ringhals BWR, while up to 59,337 metric tons are measured for the remaining Ringhals PWRs. Table 3 lists the materials that can be obtained from Ringhals NPPs. Total waste metals of 184,365 are produced from Ringhals sites, which 91.93% of these total waste metals is mainly carbon steel. The remaining small amount materials such as stainless steel (3.86%), copper (3.22%), titanium (0.87%) and other materials (0.11%) are accounted in the total metal waste productions as well.

Obviously, the amount of scrap metals generated by the decommissioning of NPP is huge, and it is possible for the scrap metals to be treated, recycled, and reused once again. This article aims to explore the possibility of using these scrap metals (low-level irradiated metals) as one of the application to control excess reactivity of light water reactors (LWRs) in form of burnable absorber material. This paper

Table 1. Ringhals Nuclear Power Plants Information

	Ringhals 1	Ringhals 2	Ringhals 3	Ringhals 4
Reactor Type	BWR	PWR	PWR	PWR
Reactor supplier	ASEA-Atom	Westinghouse Monitor AB	Westinghouse Monitor AB	Westinghouse Monitor AB
Commercial Operation	January 1976	May 1975	September 1981	November 1983
Net output (electric)	878 MWe	865 MWe	1,063 MWe	940 MWe
Thermal output	2,540 MWth	2,652 MWth	3,135 MWth	2,775 MWth
Operation Period	1976-2020	1975-2019	1981-2041	1983-2043

Table 2. Total metal wastes of Ringhals 1-4 [6]

Unit	Total weight of metal wastes (metric ton)
Ringhals 1	31,075
Ringhals 2	46,358
Ringhals 3	47,595
Ringhals 4 including unit 0	59,337
Total	184,365

Table 3. Material evaluation of Ringhals metal wastes [6]

Metals	Total weight (metric ton)
Carbon steel	169,491
Stainless steel	7,121
Copper	5,938
Titanium	1,604
Other	212
Total	184,364

studies the candidate materials of scrap metals such as carbon steel, stainless steel 304 and Inconel-718.

In light water reactors (LWRs), the burnable absorber (BA) material are used in form of rod and loaded into fuel assemblies (FAs) in order to control the FA excess reactivity. There are three types of BA that have been utilized in controlling the reactor core excess reactivity such as integral BA, discrete BA and Integral Fuel Burnable Absorber (IFBA) [7]. The integral BA type such as Gadolinium (Gd) and Erbia (Er) where BA material and fuel material are well homogeneously mixed. Gadolinium has high absorption cross section at thermal neutron energy; however, the increasing of Gadolinium content lead to increase thermal conductivity and melting point of the fuel. Erbia is used in the form of Er_2O_3 mixed with UO_2. Though, both Gadolinium and Erbia material are all depleted fast before reaching the middle of the fuel cycle. Another type of BA called discrete BA type where the burnable material and fuel material are separated in different rod, such as WABA (Wet Annual Burnable Absorber), Pyrex, and Solid Pyrex. BA material of B_4C-Al_2O_3 is used in WABA and borosilicate glass ($B_2O_3SiO_3$) is used in Pyrex and Solid Pyrex. IFBA is another BA type where its material (ZrB_2) is coated around the fuel surface. However, the neutronic characteristics of these BA types are not discussed any further.

In this paper, the nuclear characteristics of irradiated metal components such as stainless steel (SS) 304, carbon steel, and Inconel-718 are studied by examined the absorption cross section of the selected materials and analyzing on the lattice depletion calculations using Monte Carlo lattice simulations. The absorption cross section of these metal components are compared and discussed in Section 2. The lattice depletion calculations of irradiated metal components, boron content impurities within irradiated metal and the application of these irradiated metals for small reactor core are presented on Section 3. And, the Section 4 will conclude the finding as well as reviewing of the potential future works.

Table 4. The composition of fresh metal using in MCNP [10]

Fresh metal composition using in MCNP					
Fresh SS304	wt%	Fresh Carbon Steel	wt%	Fresh Inconel-718	wt%
Cr	1.30×10^{-9}	Cr	3.00×10^{-9}	B	1.00×10^{-5}
Mn	4.52×10^{-6}	Mn	8.40×10^{-7}	C	4.00×10^{-5}
Fe	9.70×10^{-8}	Fe	2.30×10^{-7}	Al	7.30×10^{-4}
Ni	1.00×10^{-6}	Ni	3.30×10^{-6}	N	5.00×10^{-3}
Li	7.00×10^{-7}	Li	4.00×10^{-7}	P	3.18×10^{-3}
Ni	3.00×10^{-8}	Ni	1.20×10^{-7}	S	1.40×10^{-4}
Na	1.90×10^{-7}	Na	1.40×10^{-7}	Ti	1.40×10^{-4}
Al	3.00×10^{-10}	Al	2.60×10^{-9}	Cr	9.00×10^{-3}
Cl	6.00×10^{-6}	Cl	2.00×10^{-8}	Mn	1.90×10^{-1}
K	4.56×10^{-6}	K	8.00×10^{-7}	Fe	3.18×10^{-3}
Ca	1.84×10^{-1}	Ca	1.70×10^{-3}	Co	1.70×10^{-1}
Sc	1.53×10^{-2}	Sc	1.02×10^{-2}	Ni	5.25×10^{-1}
Ti	7.06×10^{-1}	Ti	9.80×10^{-1}	Cu	9.10×10^{-3}
V	1.00×10^{-1}	V	6.60×10^{-3}	Nb	2.73×10^{-3}
Co	2.21×10^{-5}	Co	1.22×10^{-6}	Mo	5.13×10^{-2}
Cu	3.08×10^{-5}	Cu	1.27×10^{-5}	B	3.05×10^{-2}
Ni	4.57×10^{-6}	Ni	1.00×10^{-6}		
Ga	1.29×10^{-6}	Ga	8.00×10^{-7}		
As	1.94×10^{-6}	As	5.32×10^{-6}		
Se	3.50×10^{-7}	Se	7.00×10^{-9}		
Br	2.00×10^{-8}	Br	8.50×10^{-9}		
Rb	1.00×10^{-7}	Rb	4.80×10^{-7}		
Sr	2.00×10^{-9}	Sr	1.50×10^{-9}		
Y	5.00×10^{-8}	Y	2.00×10^{-7}		
Zr	1.00×10^{-7}	Zr	1.00×10^{-7}		
Nb	8.90×10^{-7}	Nb	1.88×10^{-7}		
Mo	2.60×10^{-5}	Mo	5.60×10^{-9}		
Ag	2.00×10^{-8}	Ag	2.00×10^{-8}		
Sb	1.23×10^{-7}	Sb	1.10×10^{-7}		
Cs	3.00×10^{-9}	Cs	2.00×10^{-9}		
Ba	5.00×10^{-6}	Ba	2.73×10^{-6}		
La	2.00×10^{-9}	La	1.00×10^{-9}		
Ce	3.71×10^{-6}	Ce	1.00×10^{-8}		
Sm	1.00×10^{-9}	Sm	2.00×10^{-10}		
Eu	4.70×10^{-9}	Eu	3.00×10^{-10}		
Tb	4.70×10^{-9}	Tb	4.50×10^{-9}		
Dy	1.00×10^{-8}	Dy	8.00×10^{-9}		
Ho	1.00×10^{-8}	Ho	1.00×10^{-8}		
Yb	2.00×10^{-8}	Yb	2.00×10^{-9}		

Fresh metal composition using in MCNP					
Fresh SS304	wt%	Fresh Carbon Steel	wt%	Fresh Inconel-718	wt%
Lu	8.00×10^{-9}	Lu	2.10×10^{-9}		
Hf	2.00×10^{-8}	Hf	1.30×10^{-9}		
W	1.86×10^{-6}	W	5.50×10^{-8}		
Pb	6.70×10^{-7}	Pb	8.20×10^{-6}		
Th	1.00×10^{-8}	Th	1.80×10^{-9}		
U	2.00×10^{-8}	U	2.00×10^{-9}		

Table 5. The composition of irradiated metal wastes using in MCNP

Irradiated SS304	wt%	Irradiated Carbon steel	wt%	Irradiated Inconel-718	wt%
^{14}N	4.502×10^{-6}	^{1}H	2.575×10^{-7}	^{1}H	1.378×10^{-7}
^{15}N	1.772×10^{-8}	^{4}He	8.571×10^{-8}	^{4}He	3.441×10^{-6}
^{23}Na	9.700×10^{-8}	^{14}N	8.355×10^{-7}	^{7}Li	5.907×10^{-6}
^{27}Al	1.000×10^{-6}	^{23}Na	2.299×10^{-7}	^{10}B	8.193×10^{-7}
^{35}Cl	5.231×10^{-7}	^{27}Al	3.299×10^{-6}	^{11}B	4.074×10^{-5}
^{37}Cl	1.769×10^{-7}	^{35}Cl	2.925×10^{-7}	^{12}C	7.212×10^{-4}
^{39}K	2.788×10^{-8}	^{37}Cl	1.011×10^{-7}	^{13}C	8.771×10^{-6}
^{40}Ca	1.837×10^{-7}	^{39}K	1.114×10^{-7}	^{25}Mg	2.523×10^{-8}
^{46}Sc	4.752×10^{-7}	^{40}Ca	1.352×10^{-7}	^{27}Al	4.999×10^{-3}
^{47}Sc	4.385×10^{-7}	^{48}Sc	1.471×10^{-8}	^{28}Si	2.922×10^{-3}
^{48}Sc	4.430×10^{-6}	^{50}Ti	1.167×10^{-8}	^{29}Si	1.535×10^{-4}
^{49}Sc	3.314×10^{-7}	^{51}Ti	1.483×10^{-6}	^{30}Si	1.052×10^{-4}
^{50}Sc	3.256×10^{-7}	^{50}Cr	7.044×10^{-5}	^{31}P	1.400×10^{-4}
^{50}Ti	1.225×10^{-8}	^{52}Cr	1.422×10^{-3}	^{32}S	1.326×10^{-4}
^{51}Ti	4.613×10^{-6}	^{53}Cr	1.644×10^{-4}	^{33}S	1.133×10^{-6}
^{50}Cr	7.688×10^{-3}	^{54}Cr	5.338×10^{-5}	^{34}S	6.248×10^{-6}
^{52}Cr	1.540×10^{-1}	^{55}Mn	1.016×10^{-2}	^{36}S	2.670×10^{-8}
^{53}Cr	1.780×10^{-2}	^{54}Fe	5.492×10^{-2}	^{46}Sc	7.125×10^{-4}
^{54}Cr	4.505×10^{-3}	^{56}Fe	8.995×10^{-1}	^{47}Sc	6.572×10^{-4}
^{55}Mn	1.530×10^{-2}	^{57}Fe	2.271×10^{-2}	^{48}Sc	6.618×10^{-3}
^{54}Fe	3.962×10^{-2}	^{58}Fe	2.977×10^{-3}	^{49}Sc	5.237×10^{-4}
^{56}Fe	6.488×10^{-1}	^{59}Co	3.725×10^{-6}	^{50}Sc	4.889×10^{-4}
^{57}Fe	1.548×10^{-2}	^{58}Ni	4.436×10^{-3}	^{50}Ti	1.091×10^{-6}
^{58}Fe	2.124×10^{-3}	^{59}Ni	1.045×10^{-5}	^{51}Ti	6.578×10^{-5}
^{59}Co	2.214×10^{-5}	^{60}Ni	$1.757\times1^{0-3}$	^{50}Cr	7.873×10^{-3}
^{58}Ni	6.740×10^{-2}	^{61}Ni	7.993×10^{-5}	^{52}Cr	1.590×10^{-1}
^{59}Ni	1.644×10^{-7}	^{62}Ni	2.483×10^{-4}	^{53}Cr	1.828×10^{-2}
^{60}Ni	2.665×10^{-2}	^{63}Ni	6.540×10^{-5}	^{54}Cr	4.824×10^{-3}
^{61}Ni	1.173×10^{-3}	^{63}Cu	8.990×10^{-6}	^{55}Mn	3.159×10^{-3}

Irradiated SS304	wt%	Irradiated Carbon steel	wt%	Irradiated Inconel-718	wt%
^{62}Ni	3.788×10^{-3}	^{65}Cu	4.058×10^{-6}	^{54}Fe	9.526×10^{-3}
^{63}Ni	9.913×10^{-4}	^{64}Zn	4.847×10^{-7}	^{56}Fe	1.560×10^{-1}
^{63}Cu	2.111×10^{-5}	^{66}Zn	2.871×10^{-7}	^{57}Fe	3.939×10^{-3}
^{65}Cu	9.694×10^{-6}	^{67}Zn	4.176×10^{-8}	^{58}Fe	5.178×10^{-4}
^{69}Ga	7.664×10^{-7}	^{68}Zn	1.952×10^{-7}	^{58}Co	4.552×10^{-24}
^{71}Ga	5.236×10^{-7}	^{69}Ga	4.732×10^{-7}	^{59}Co	5.049×10^{-1}
^{75}As	1.940×10^{-6}	^{71}Ga	3.213×10^{-7}	^{58}Ni	6.117×10^{-3}
^{76}Se	3.041×10^{-8}	^{75}As	5.230×10^{-6}	^{59}Ni	1.441×10^{-5}
^{77}Se	2.590×10^{-8}	^{76}Se	8.932×10^{-8}	^{60}Ni	2.146×10^{-2}
^{78}Se	8.113×10^{-8}	^{85}Rb	3.435×10^{-7}	^{61}Ni	1.245×10^{-4}
^{80}Se	1.763×10^{-7}	^{87}Rb	1.357×10^{-7}	^{62}Ni	3.424×10^{-4}
^{82}Se	3.339×10^{-8}	^{89}Y	1.999×10^{-7}	^{63}Ni	9.374×10^{-5}
^{85}Rb	7.170×10^{-8}	^{90}Zr	5.091×10^{-8}	^{63}Cu	1.866×10^{-3}
^{87}Rb	2.830×10^{-8}	^{91}Zr	1.115×10^{-8}	^{65}Cu	8.580×10^{-4}
^{89}Y	5.000×10^{-8}	^{92}Zr	1.724×10^{-8}	^{64}Zn	2.121×10^{-6}
^{90}Zr	5.076×10^{-8}	^{94}Zr	1.791×10^{-8}	^{66}Zn	1.272×10^{-6}
^{91}Zr	1.116×10^{-8}	^{93}Nb	1.874×10^{-7}	^{92}Zr	1.635×10^{-8}
^{92}Zr	1.723×10^{-8}	^{121}Sb	6.012×10^{-8}	^{93}Zr	7.605×10^{-8}
^{94}Zr	1.791×10^{-8}	^{123}Sb	4.603×10^{-8}	^{93}Nb	5.109×10^{-2}
^{93}Nb	8.900×10^{-7}	^{134}Ba	6.358×10^{-8}	^{94}Nb	1.589×10^{-4}
^{92}Mo	3.687×10^{-6}	^{135}Ba	1.727×10^{-7}	^{95}Nb	1.357×10^{-29}
^{94}Mo	2.367×10^{-6}	^{136}Ba	2.181×10^{-7}	^{92}Mo	4.323×10^{-3}
^{95}Mo	4.090×10^{-6}	^{137}Ba	3.042×10^{-7}	^{94}Mo	2.776×10^{-3}
^{96}Mo	4.341×10^{-6}	^{138}Ba	1.966×10^{-6}	^{95}Mo	4.657×10^{-3}
^{97}Mo	2.521×10^{-6}	^{182}W	1.271×10^{-8}	^{96}Mo	5.209×10^{-3}
^{98}Mo	6.395×10^{-6}	^{184}W	1.745×10^{-8}	^{97}Mo	2.971×10^{-3}
^{100}Mo	2.599×10^{-6}	^{186}W	1.404×10^{-8}	^{98}Mo	7.504×10^{-3}
^{107}Ag	1.027×10^{-8}	^{204}Pb	1.129×10^{-7}	^{100}Mo	3.046×10^{-3}
^{121}Sb	6.998×10^{-8}	^{206}Pb	1.964×10^{-6}	^{99}Tc	1.384×10^{-5}
^{123}Sb	5.301×10^{-8}	^{207}Pb	1.810×10^{-6}	^{100}Ru	4.535×10^{-7}
^{134}Ba	1.170×10^{-7}	^{208}Pb	4.313×10^{-6}	^{101}Ru	3.533×10^{-6}
^{135}Ba	3.237×10^{-7}			^{102}Ru	4.411×10^{-8}
^{136}Ba	3.909×10^{-7}				
^{137}Ba	5.583×10^{-7}				
^{138}Ba	3.600×10^{-6}				
^{140}Ce	3.278×10^{-6}				
^{142}Ce	4.163×10^{-7}				
^{175}Lu	1.947×10^{-8}				
^{181}Ta	1.999×10^{-8}				
^{182}W	4.841×10^{-7}				
^{183}W	2.647×10^{-7}				

Irradiated SS304	wt%	Irradiated Carbon steel	wt%	Irradiated Inconel-718	wt%
^{184}W	5.708×10^{-7}				
^{186}W	5.380×10^{-7}				
^{206}Pb	1.605×10^{-7}				
^{207}Pb	1.479×10^{-7}				
^{208}Pb	3.524×10^{-7}				

Table 6. The total activity of irradiated metal components in $Bq\cdot g^{-1}$

Irradiated SS304		Irradiated CS		Irradiated Inconel-718	
^{110m}Ag	2.66×10^{-2}	^{110m}Ag	3.40×10^{-3}	^{110m}Ag	1.53×10^{-19}
^{14}C	8.34×10^{2}	^{14}C	8.34×10^{1}	^{14}C	2.14×10^{0}
^{45}Ca	7.16×10^{-6}	^{45}Ca	7.17×10^{-7}	^{45}Ca	2.14×10^{-3}
^{109}Cd	1.61×10^{-2}	^{109}Cd	1.67×10^{-4}	^{109}Cd	1.87×10^{-22}
^{139}Ce	5.73×10^{-7}	^{139}Ce	5.76×10^{-8}	^{136}C	9.61×10^{-3}
^{144}Ce	4.07×10^{-7}	^{144}Ce	4.30×10^{-9}	^{58}Co	5.35×10^{-9}
^{136}C	1.40×10^{1}	^{36}Cl	1.42×10^{0}	^{60}Co	5.65×10^{10}
^{58}Co	4.69×10^{-8}	^{58}Co	4.86×10^{-9}	^{55}Fe	1.09×10^{7}
^{60}Co	3.01×10^{6}	^{60}Co	2.90×10^{5}	^{3}H	1.69×10^{2}
^{134}Cs	3.54×10^{1}	^{134}Cs	3.57×10^{0}	^{42}K	7.79×10^{-6}
^{135}Cs	7.21×10^{-4}	^{135}Cs	6.83×10^{-5}	^{54}Mn	6.27×10^{3}
^{137}Cs	1.01×10^{-4}	^{137}Cs	1.06×10^{-7}	^{93}Mo	6.45×10^{4}
^{152}Eu	7.11×10^{2}	^{152}Eu	3.81×10^{1}	^{22}Na	2.02×10^{-12}
^{154}Eu	1.11×10^{3}	^{154}Eu	7.35×10^{0}	^{93m}Nb	1.81×10^{7}
^{155}Eu	1.29×10^{2}	^{155}Eu	3.76×10^{-1}	^{94}Nb	1.10×10^{6}
^{55}Fe	4.62×10^{7}	^{55}Fe	4.63×10^{6}	^{95}Nb	1.97×10^{-14}
^{153}Gd	6.69×10^{-3}	^{153}Gd	1.28×10^{-5}	^{59}Ni	4.31×10^{4}
^{3}H	2.57×10^{3}	^{3}H	2.29×10^{2}	^{63}Ni	4.57×10^{6}
^{129}I	2.35×10^{-13}	^{129}I	2.29×10^{-15}	^{32}P	7.69×10^{-3}
^{192}Ir	1.10×10^{-8}	^{192}Ir	1.70×10^{-14}	^{106}Ru	6.17×10^{-15}
^{194}Ir	1.88×10^{-14}	^{42}K	3.18×10^{-10}	^{35}S	3.67×10^{-9}
^{42}K	3.17×10^{-8}	^{177}Lu	2.32×10^{-8}	^{46}Sc	1.64×10^{-8}
^{177}Lu	3.13×10^{-7}	^{54}Mn	2.61×10^{3}	^{90}Sr	1.71×10^{-2}
^{54}Mn	2.60×10^{4}	^{93}Mo	5.52×10^{0}	^{97}Tc	4.01×10^{-9}
^{93}Mo	5.50×10^{1}	^{22}Na	1.88×10^{-4}	^{99}Tc	8.76×10^{3}
^{22}Na	7.65×10^{-4}	^{93m}Nb	3.42×10^{1}	^{90}Y	1.72×10^{-2}
^{93m}Nb	3.42×10^{2}	^{94}Nb	1.94×10^{0}	^{91}Y	1.23×10^{-20}
^{94}Nb	1.91×10^{-1}	^{95}Nb	3.02×10^{-19}	^{93}Zr	7.07×10^{0}
^{95}Nb	2.72×10^{-16}	^{59}Ni	4.90×10^{4}	^{95}Zr	8.96×10^{-15}
^{59}Ni	4.73×10^{5}	^{63}Ni	4.90×10^{6}		
^{63}Ni	4.86×10^{7}	^{185}Os	3.64×10^{-17}		
^{185}Os	3.17×10^{-14}	^{32}P	1.51×10^{-7}		

Irradiated SS304		Irradiated CS		Irradiated Inconel-718
^{32}P	1.49×10^{-5}	^{147}Pm	2.76×10^{-7}	
^{147}Pm	2.90×10^{-6}	^{106}Ru	1.66×10^{-18}	
^{188}Re	1.46×10^{-16}	^{35}S	2.54×10^{-11}	
^{106}Ru	1.57×10^{-15}	^{124}Sb	4.36×10^{-16}	
^{35}S	2.49×10^{-10}	^{125}Sb	5.00×10^{-4}	
^{124}Sb	4.25×10^{-15}	^{46}Sc	1.54×10^{-12}	
^{125}Sb	4.88×10^{-2}	^{75}Se	2.64×10^{-7}	
^{46}Sc	1.54×10^{-11}	^{151}Sm	1.30×10^{0}	
^{75}Se	2.28×10^{-6}	^{90}Sr	2.07×10^{-8}	
^{151}Sm	4.42×10^{0}	^{182}Ta	1.92×10^{-9}	
^{113}Sn	1.63×10^{-23}	^{160}Tb	1.32×10^{-13}	
^{89}Sr	6.40×10^{-23}	^{97}Tc	3.61×10^{-15}	
^{90}Sr	2.07×10^{-6}	^{99}Tc	7.83×10^{-1}	
^{182}Ta	2.33×10^{-6}	^{123m}Te	6.89×10^{-10}	
^{160}Tb	1.20×10^{-12}	^{125m}Te	1.22×10^{-4}	
^{97}Tc	3.42×10^{-12}	^{127m}Te	1.68×10^{-19}	
^{99}Tc	7.47×10^{0}	^{204}Tl	5.23×10^{-6}	
^{123m}Te	6.59×10^{-8}	^{170}Tm	2.14×10^{-9}	
^{125m}Te	1.19×10^{-2}	^{171}Tm	5.76×10^{-6}	
^{127}Te	1.63×10^{-15}	^{181}W	5.19×10^{-8}	
^{127m} Te	1.66×10^{-15}	^{185}W	2.37×10^{-12}	
^{204}Tl	5.45×10^{-5}	^{90}Y	2.07×10^{-8}	
^{170}Tm	3.84×10^{-8}	^{91}Y	6.87×10^{-22}	
^{171}Tm	1.01×10^{-3}	^{65}Zn	5.48×10^{-5}	
^{181}W	4.85×10^{-7}	^{93}Zr	7.13×10^{-5}	
^{185}W	2.44×10^{-11}	^{95}Zr	1.23×10^{-17}	
^{90}Y	2.07×10^{-6}			
^{91}Y	6.90×10^{-21}			
^{93}Zr	7.12×10^{-4}			
^{95}Zr	1.23×10^{-16}			
Total Activity (Bq·g^{1})	9.83×10^{7}		9.87×10^{6}	5.66×10^{10}

2. Computer Codes, Model and Analysis Conditions

The nuclide compositions of the irradiated metals were generated using ORIGEN-ARP [8]. The nuclide depletion calculation of ORIGEN is calculated for Westinghouse (WH) 17×17 fuel assembly. The irradiated metals are irradiated in NPP about 40 years and cooled down for about 10 years. For one fuel assembly, the total neutron flux level is 1×10^{12} n cm^{-2}·s^{-1}. The compositions of fresh and irradiated waste metals are calculated and given in Table 4 and Table 5, respectively. The total activity of irradiated metal components also obtained from ORIGEN-ARP output [9]. The total activity of the irradiated Inconel-718 is 5.66×10^{10} Bq·g^{-1}, the irradiated SS304 is 9.83×10^{7} Bq·g^{-1} and the irradiated carbon steel is 9.87×10^{6} Bq·g^{-1}, respectively. The

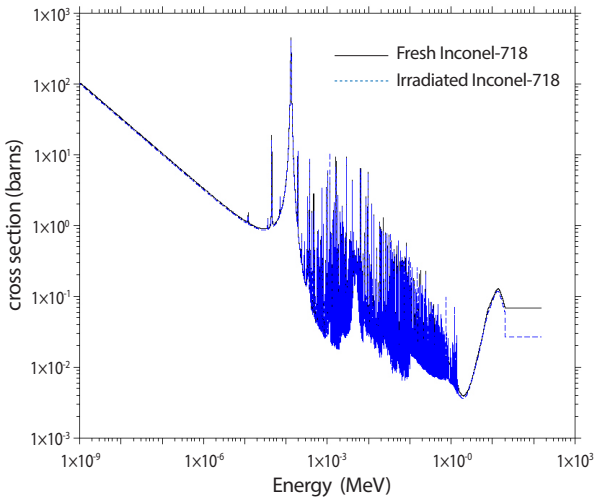

Fig. 1. Absorption cross section of fresh and irradiated Inconel-718.

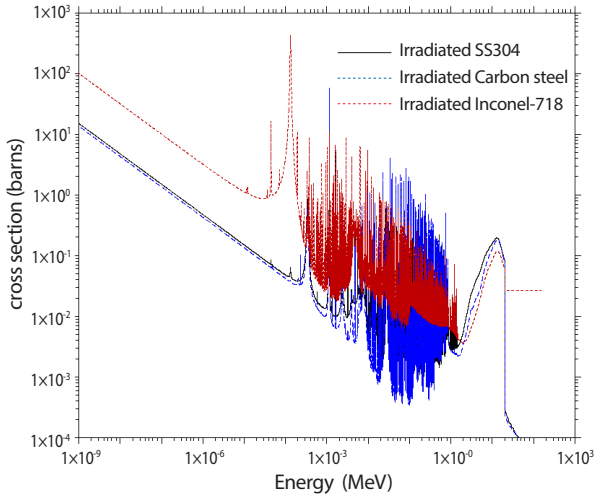

Fig. 2. Absorption cross section of irradiated metal wastes.

total activity of irradiated Inconel-718 is higher than SS304 and carbon steel. The total activity of ^{60}Co was observed to be 5.65×10^{10} Bq·g^{-1}, which accounted for the most inside the irradiated Incondel-718.

2.1 Absorption crosssection comparison

The examination of neutron absorption crosssections of irradiated metals is conducted in order to investigate its absorption capability. The comparison of fresh and irradiated Inconel-718 absorption crosssection is depicted in Fig. 1. It was observed that even after 40 years of being irradiated in NPPs, the neutron absorption crosssection of Inconel-718 seems wellmaintained and in near perfect condition. Fig. 2 displays the neutron absorption crosssection of other irradiated metals such as SS304, carbon steel, and Inconel-718. The irradiated Inconel-718 has the higher neutron absorption crosssection at thermal region than that to the other two irradiated metals. The irradiated Inconel-718 has a high thermal neutron absorption cross section, showing incredible potential and can be suitable used as an absorber material to control reactivity of fuel assembly or reactor core. In this paper, it was assumed that the irradiated metals are affordable and available to be used as BA material.

2.2 Fuel assembly and BA assembly descriptions

A typical Westinghouse (WH) 17×17 fuel assembly (FA) has 264 fuel rods, 24 guide tubes, and one instrument tube which is chosen for the depletion analysis. WH 17×17 FA crosssectional view is shown in Fig. 3 and its design description is presented in Table 7. The fuel enrichment of ^{235}U of 4.95wt% is utilized in the depletion calculation. The location of BA loaded within FA is displayed in Fig. 3. There are 24 BA rods placed near waterhole tubes. As mentioned earlier, there are three different types of BA which have been utilized in LWRs such as integral BA ($UO_2Gd_2O_3$, $UO_2Er_2O_3$), discrete BA (WABA, Pyrex, Solid Pyrex) and IFBA (ZrB_2). Moreover, another geometric design similar to discrete BA, is called SLOBA (slow burnable absorber). In this paper, the loaded BA rod FA using SLOBA geometry for depletion simulation has been considered. The optimum crosssectional configuration of SLOBA geometry and its dimensions are displayed in Fig. 4. The details of nuclear characteristics of SLOBA and its applications for soluble boron free core of small modular reactor application can be found in [7] and [11, 12]. These studies show the application of controlling power

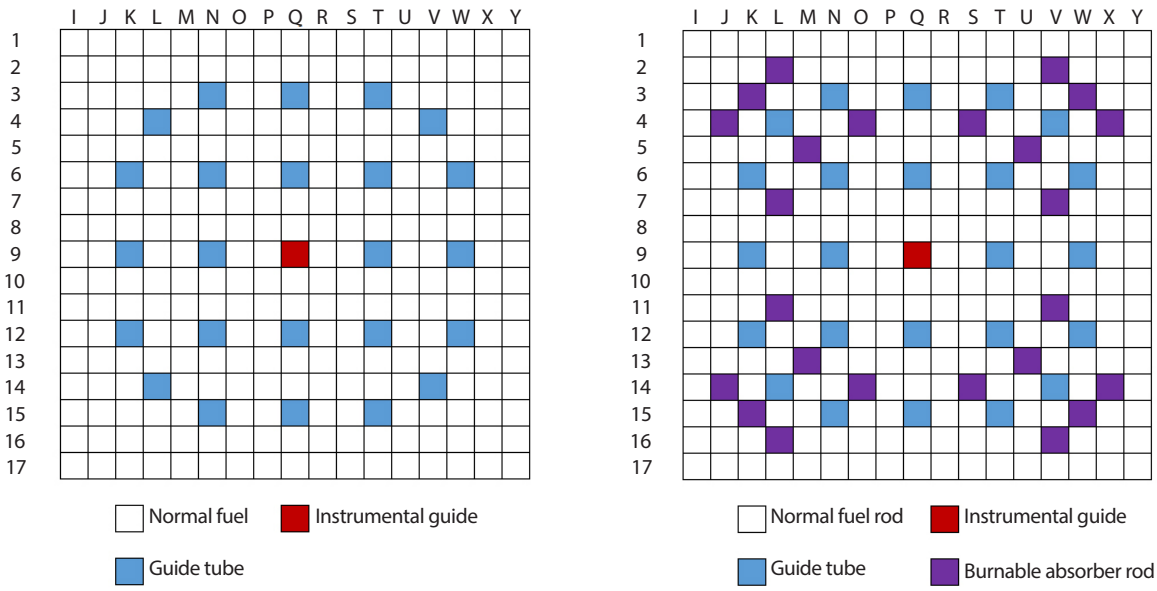

Fig. 3. Configuration of WH 17×17 FA and loaded BA rod within FA.

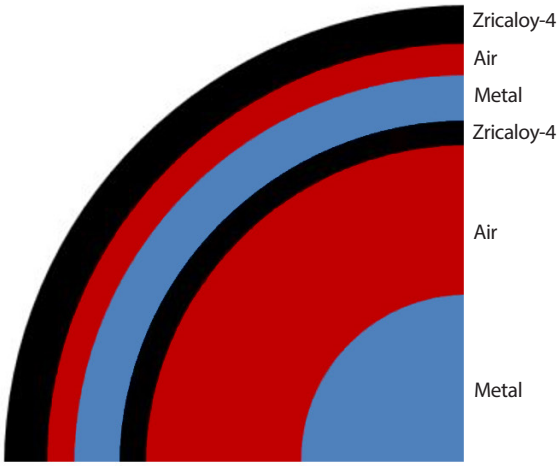

Region	Radius (cm)	Thickness (cm)	Material
1	0.2000	0.2000	Metal components
2	0.3750	0.1750	Air
3	0.3800	0.0050	Zircaloy - 4
4	0.4100	0.0300	Metal components
5	0.4316	0.0216	Air
6	0.4760	0.0444	Zircaloy - 4

Fig. 4. Optimum configuration of burnable absorber and its dimensions.

distribution and pin power factor of epithermal nuclear icepower breaker reactor.

The lattice depletion calculation of WH 17×17 FA array with and without BA rod has been performed using MCNP code with ENDF/BVII.1 neutron cross section library [13]. To determine the infinite multiplication factor (kinf) of FA, KCODE card has been employed, which accounts for 5,000 neutron histories, 250 active cycles, and 50 inactive cycles. A small number of neutron histories has been chosen to reduce the computation time and to investigate the trend of kinf curve of the proposed irradiated metal components. BURN card has been employed which contains information such as TIME (time steps for depletion in increment), PFRAC (fraction of total system power), Power (system power in MWth), MAT (material number to be burned), OMIT (specific isotopes to be omit

Table 7. The design parameters of WH 17×17 fuel assembly

Fuel assembly Parameters	Dimension	Value
Fuel composition		UO_2 (enriched 4.95wt% of ^{235}U)
Fuel density	$g \cdot cm^{-3}$	10.412
Number of fuel rod		264
Number of guide tube		24
Number of instrumentation tube		1
Fuel rod ID radius	cm	0.4095
Fuel rod OD radius	cm	0.4750
Pin pitch	cm	1.2540
Assembly pitch	cm	21.318
Guide tube ID radius	cm	0.5700
Guide tube OD radius	cm	0.6100

Noted: ID = Inner diameter
OD = Outer diameter

from specific material number), MATVOL (material volume to be burned) and BOPT (controlling parameters).

3. Lattice Depletion Analysis

3.1 Depletion calculation of irradiated metal components

The density of irradiated Inconel-718 is 8.19 $g \cdot cm^{-3}$, SS304, 7.87 $g \cdot cm^{-3}$ and carbon steel, 7.82 $g \cdot cm^{-3}$, respectively, have been used for the whole simulation. The density of those irradiated metals has the exactly the same value to the fresh metals. The result of the depletion calculation of irradiated metal wastes comparing to the fresh FA kinf is shown in Fig. 5 which corresponds to the kinf value at BOC (beginning of cycle) and EOC (end of cycle), the percentage of kinf difference of BOC to EOC is shown in Table 8. The depletion calculation is simulated at room temperature. Judging from the absorption crosssection of the irradiated Inconel-718, it is not surprising that the kinf of fresh FA is significantly reduced, while the irradiated SS304 and

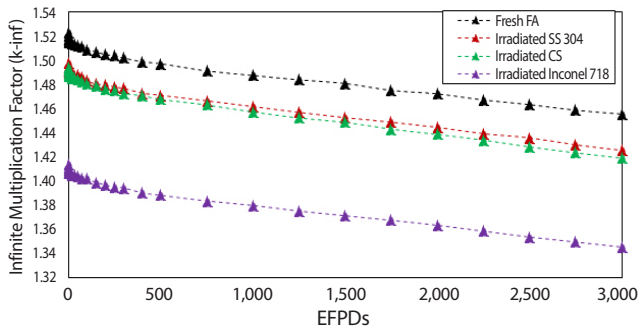

Fig. 5. The depletion calculation of irradiated metal components and fresh FA.

Table 8. The kinf differences of fresh FA vs irradiated metal wastes

Cases	BOC kinf	EOC kinf.	%Δk[a]
Fresh FA	1.52309	1.45563	6.746
Irradiated Inconel-718	1.41420	1.34549	6.871
Irradiated SS304	1.49799	1.42559	7.240
Irradiated carbon steel	1.49416	1.41916	7.500

[a] reactivity difference between BOC to EOC in percentage

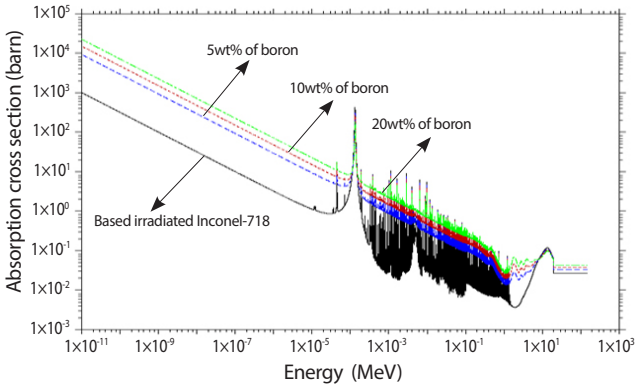

Fig. 6. The absorption cross section of boron content added into the irradiated Inconel-718.

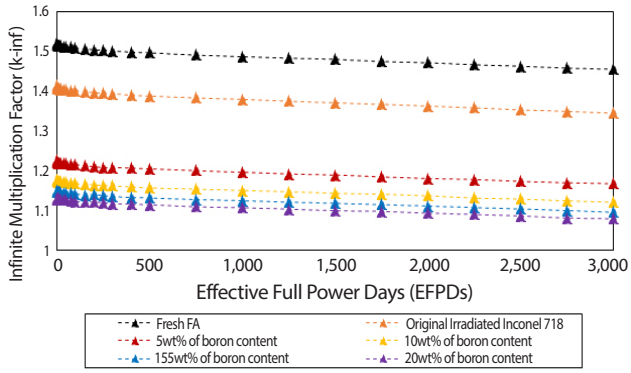

Fig. 7. The kinf variation of boron content in irradiated Inconel-718.

Table 9. The kinf difference of boron content variations of the irradiated Inconel-718

Cases	BOC kinf	EOC kinf	%Δk
Based Irradiated Inconel-718	1.41420	1.34549	6.871
5wt% of boron	1.22587	1.16788	5.799
10wt% of boron	1.17810	1.12137	5.673
15wt% of boron	1.15084	1.09601	5.483
20wt% of boron	1.13139	1.07961	5.178

carbon steel have a lower inhibition effect on the fresh FA excess reactivity. It should be noted that fresh and irradiated Inconel-718 contains small amount of neutron absorbing material, Boron (about 4.16E7 in weight percentwt%). If the boron added to Inconel-718, the FA excess reactivity may be further reduced greater.

3.2 The impurity of boron concentration in Inconel-718

As mentioned before, the fresh and irradiated Inconel-718 contain a small amount of boron content. Therefore, the investigation of boron content additive to irradiated Inconel-718 is conducted to investigate the effect of burnable material. The added boron is examined from 5wt% to 20wt% in irradiated Inconel-718. The natural boron which has two isotopes occurring naturally, ^{10}B with 19.1wt% (abundant) and ^{11}B with 89.9wt%, is adopted in the calculation. Before starting the depletion calculation, the absorption ability of the added boron contents in irradiated Inconel-718 has been investigated and the result is plotted in Fig. 6. Apparently, as the boron contents increase within the irradiated Inconel-718, the irradiated Inconel-718 absorption crosssection is enhanced and improved. Fig. 7 shows the depletion calculation of different boron contents from 5wt% to 20wt% added to irradiated Inconel-718 compared to fresh fuel assembly and the original of irradiated Inconel-718. The criticality and depletion calculation are done for 3000 days of lattice depletion. It was found that the increased boron content of irradiated Inconel-718 results in a significant reduction in excess reactivity of the FA. The corresponding%Δk between BOC and EOC of all case of the boron content added to the irradiated Inconel-718 is presented in Table 9. The reactivity difference%Δk of 5wt% is 5.80%Δk; 10wt% is 5.67%Δk; 15wt% is 5.48%Δk, 20wt% is 5.18%Δk, respectively. The variation in the

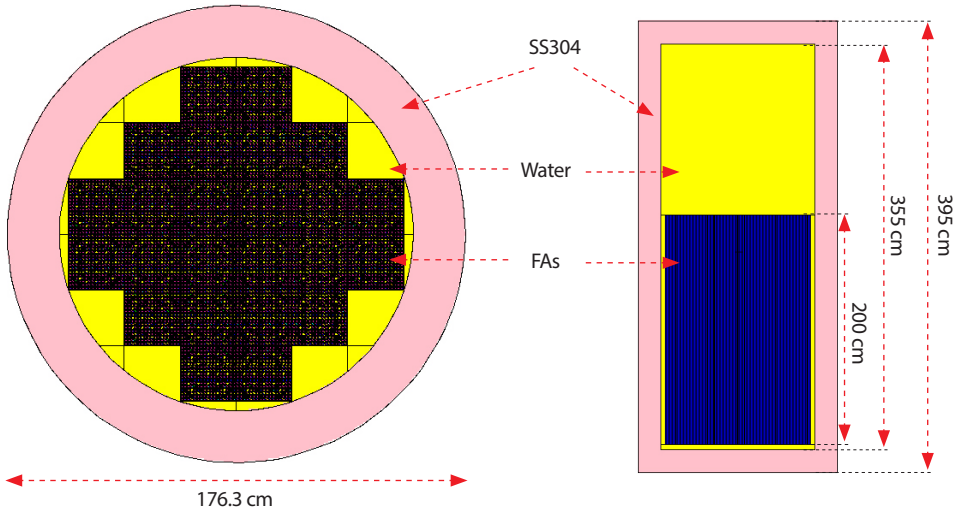

Fig. 8. Cross sectionalviews of small modular reactor.

reactivity in each case is decreasing while the boron content keeps increasing within the irradiated Inconel-718. It may be possible to consider higher boron content added to irradiated Inconel-718 to provide a smaller reactivity swing. However, if the huge amount of boron content is added to irradiated Inconel-718, the irradiated Inconel-718 may lose its chemical property as well as other nuclear characteristics such as absorption or capture crosssection. This matter should be investigated further in details.

3.3 Application of irradiated Inconel-718 for small modular reactor concept

The application of irradiated Inconel-718 as burnable absorber is proposed as one of the reactivity controlling system in a small modular reactor (SMR) core. The SMR core consists of 24 WH 17×17 FA which each FA is loaded with 24 BA rods. The vertical and horizzontal crosssectional view of the proposed SMR is shown in Fig. 8. The SMR is operated at 100 MWth thermal power (each FA has the thermal power of 4.16 MWth). The active fuel assembly height of 200 cm is considered. The core is surrounding with light water. The reactor vessel is made of stainless steel 304 (SS304) with the thickness of 20 cm at top, bottom and side of reactor vessel. This SMR core has a diameter of 176.3 cm and total height of 395 cm. The region above the fuel is filled with water to accommodate the control rod movement. However, the control rod mechanism is not considered in this study. The depletion calculation of SMR core is investigated with the four distinguished cases as follows:

1) Case 1: core depletion at room temperature, all FAs are not loaded with BA
2) Case 2: core depletion at room temperature, all FAs loaded with 24 BA rods (the irradiated Inconel-718 has boron content of 20wt%)
3) Case 3: core depletion at the dependent temperature of material composition is at 600 K which all FAs are not loaded with BA
4) Case 4: core depletion at the dependent temperature of material composition is at 600 K, all FAs loaded with 24 BA rods (the irradiated Inconel-718 has boron content of 20wt%)

To obtain accuracy and small value of standard deviation in MCNP simulation, the neutron histories of 30,000, 50 inactive cycles and 200 active cycles are chosen for performing the whole core depletion simulation for 2,000 effective full power days (EFPDs). The simulation result of

Table 10. The kinf difference of four study cases to investigate the temperature dependence

Cases	BOC kinf	EOC kinf	%Δk
CASE 1	1.42269	1.10114	32.155
CASE 2	1.06424	0.84293	22.131
CASE 3	1.30512	1.01404	29.108
CASE 4	0.91928	0.79731	12.197

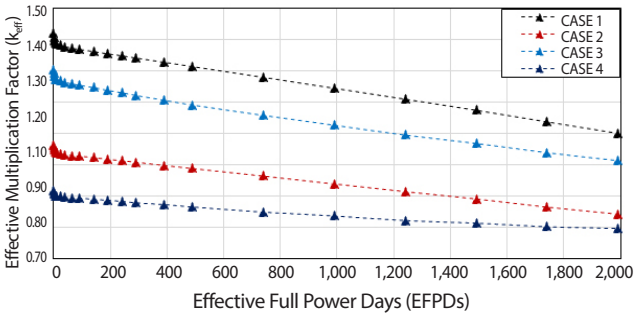

Fig. 9. The whole depletion calculation of four cases to investigate the temperature dependence.

four study cases is illustrated in Fig. 9.

Fig. 9 shows the depletion calculation of the four study cases, which illustrates the variation of effective multiplication factor (keff) against the effective full power days (EFPDs). Table 10 summaries the keff at BOC and at EOC, as well as the %Δk of each case. The 1st and 2nd cases are depleted and analyzed for the whole core material at the room temperature. At room temperature, the 1st case has the highest core reactivity at the BOC. The 3rd case analytical condition is exactly the same to the 1st case except the temperature of all material composition is set at 600 K. The %Δk of the 1st case compared to the 3rd case is about 11.75% at the BOC and 8.71% at EOC. The temperature dependence of material composition of the whole core depletion calculation at 600 K is clearly influencing the core reactivity. The 2nd case is the depletion calculation when all fuel assemblies loaded with 24 BA rods (each BA rod contains irradiated Inconel-718 with impurity of 20wt% of boron content) at room temperature for all material composition. The reactivity reduction of the reactor core of 1st case without BA loaded compared to the reactor core with BA loaded of the 2nd case is about 35.87%Δk at BOC and 25.81%Δk at EOC. The impurity boron content added to irradiated Inconel-718 has significantly enhanced the core reactivity suppression. As shown in Fig. 9 and Table 10, the last two cases are conducted to study the temperature dependence affected on the core reactivity compared to the 1st and the 2nd case. The curves of the 3rd and the 4th cases are presented the core reactivity trend at 600 K temperature, where the %Δk between 3rd and 4th case is 38.58%Δk at BOC and 21.67%Δk. Obviously, the temperature dependence of material compositions of between 3rd and 4th case show a huge reactivity than that between 1st and 2nd case of the whole core without using BA compared to the whole core using BA.

The whole core depletion calculation of four cases did not aim to achieve criticality but rather to investigate the effect of temperature on material composition of each case. To achieve criticality as well as low reactivity, the reactor core loading pattern is needed to construct to achieve optimum desirable and operational condition.

4. Conclusion

A huge quantity of irradiated metal wastes from NPP decommissioning still has economical value after recycling, and these metals can be used again. It is considered that these waste metals can be used as neutron absorber material in typical LWRs. The investigation of irradiated waste metals such as SS304, carbon steel, and Inconel-718 nuclear characteristics as burnable absorber materials has

been proposed. Therefore, the examination of absorption capability of these metals is performed by investigating the absorption crosssections of these metals before and after irradiated within nuclear power plants. From the results, the absorption crosssections of irradiated metal wastes are still wellmaintained even after over 40 years of irradiation.

It was found that the irradiated Inconel-718 has higher capture crosssection compared to SS304 and carbon steel at thermal neutron energy. After analyzing the lattice depletion calculation of the three proposed irradiated metals, the irradiated Inconel-718 demonstrates the advantage in controlling fuel assembly excess reactivity compared to the other two irradiated waste metals, because of the existence of small quantity of boron content within irradiated Inconel-718. Therefore, the sensitivity study of impurity of boron content added to the irradiated Inconel-718 is also carried out. It was found that the increase of boron content to irradiated Inconel-718 improves its performance in term of FA excess reactivity inhibition. Furthermore, irradiated Inconel-718 is used for a proposed SMR core consisted of 24 FAs in order to evaluate the application of irradiated Inconel-718 as burnable absorber material. Four cases of whole core depletion calculation are investigated the depletion calculation at room temperature and at 600 K of the core without loaded BA and with loaded BA. The results are summaries as following:

1) The %Δk between 1st and 2nd case is quite higher than that to the %Δk between 3rd and 4th case at BOC and EOC. The temperature crosssection dependence should apply for all cases to study further.
2) The 4th case shows a reactivity difference of 12.19%Δk lower than that to the other cases. The various number of BA rods loaded to FA should investigate further to achieve optimum loading pattern.

The further works of key neutronic parameters such as the optimization of core loading pattern, the implementation of control rod mechanism, the radial and the axial power distribution analysis, reactivity temperature coefficients and safety margin of the proposed SMR, are under constructed to evaluate the possibility of irradiated Inconel-718 application as burnable absorber.

Acknowledgement

This work was supported by the Korea Research Fund (KRF) and the Ministry of Science and ICT (MSIT) of the Republic of Korea (No. 2020M2A8A402385613).

.

REFERENCES

[1] A. Slimák and V. Nečas, “Melting of contaminated metallic materials in the process of the decommissioning of nuclear power plants”, Prog. Nucl. Energy, 92, 29-39 (2016).
[2] T. Hrncir and V. Necas, “Recyling and reuse of very low level radiactive stell in motorway tunnel scenario”, Nucl. Eng. Des., 265, 534-541 (2013).
[3] Nuclear Energy Agency of the OECD. Recycling and reuse of Scrap Metals, OECD, Paris (1996).
[4] Nuclear Energy Agency of the OECD. Recycling and Reuse of Materials Arising from the Decommissioning of Nuclear Facilities, Nuclear Energy Agency Report, NEA-7310 (2017).
[5] International Atomic Energy Agency. Application of Thermal Technologies for Processing of Radioactive Waste, International Atomic Energy Agency Report, IAEATECDOC-1527 (2006).
[6] T. Hansson, T. Norberg, A. Knutsson, P. Fors, and C. Sandebert. Ringhals Site Study 2013-An Assessment of the decommissioning cost for the Ringhals site, Svensk Kärnbränslehantering AB Technical Report, SKB-R-13-05 (2013).
[7] P. Jinha, K. JungKil, and H. ChangJoo, “Reactivity Flattening for a Soluble BoronFree Small Modular Reactor”, KINGS (KEPCO International Nuclear Graduate School), M.E. Dissertation (2015).

[8] I. Gauld, S. Bowman, and J. Horwedel. ORIGENARP: Automatic Rapid Processing for Spent Fuel Depletion, Decay, and Source Term Analysis, Oak Ridge National Laboratory Report, ORNL/TM2005/39 (2011).

[9] J. Evans, E. Lepel, R. Sanders, C. Wikerson, W. Silker, C. Thomas, K. Abel, and D. Robertson. Long Lived Activation Products in Reactor Materials, Pacific Northwest Laboratory Report, NUREG/CR-3474 (1984).

[10] R. McConn, C. Gesh, R. Pagh, R. Rucker, and R. Williams. Radiation Portal Monitoor Project Compendium of Material Composition Data for Radiation Transport Modeling, Pacific Northwest Notional Laboratory Report, PNNL-15870 (2011).

[11] M. Boravy, "Parametric Study on Burnable Absorber Rod to Control Excess Reactivity for a Soluble Boron Free Small Modular Reactor", KINGS (KEPCO International Nuclear Graduate School), M.E. Dissertation (2016).

[12] M. Boravy and C.J. Hah, "Application of B_4C/Al_2O_3 burnable absorber rod to control the excess reactivity of SMR", Transaction of the Korean Nuclear Society Autumn Meeting (2016).

[13] D.B. Pelowitz. MCNP6TM User's Manual Version 1.0, Los Alamos National Laboratory Report, LA-CP-13-00634 (2013).